# Ring-shear test data of quartz sand SIBELCO S80 used for analogue modelling in the Tectonic Laboratory (TecLab) at Utrecht University (https://doi.org/10.5880/fidgeo.2025.024)

Ernst Willingshofer[1], Matthias Rosenau*[2]

1. *Department of Earth Sciences, Utrecht University, Utrecht, The Netherlands*
2. *GFZ Helmholtz Centre for Geosciences, Potsdam, Germany*

** Corresponding author: rosen@gfz-potsdam.de*

## 1. Licence



## 2. Citation

When using the data please cite:

Willingshofer, Ernst; Rosenau, Matthias (2024): Ring-shear test data of quartz sand SIBELCO S80 used for analogue modelling in the Tectonic Laboratory (TecLab) at Utrecht University. GFZ Data Services. https://doi.org/10.5880/fidgeo.2025.024

## Table of contents



## 3. Data description

This dataset provides friction data from ring-shear tests on quartz sand SIBELCO S80 used in analogue modelling of tectonic processes as a rock analogue for the earth's upper crust (e.g., Klinkmüller et al., 2016).

According to our analysis the material shows a Mohr-Coulomb behaviour characterized by a linear failure envelope. Peak, dynamic and reactivation friction coefficients of quartz sand S80 are $\mu_P$ = 0.75,

$\mu_D$ = 0.59, and $\mu_R$ = 0.69, respectively (Table 5). Cohesion of the material ranges between 0-80 Pa. The material shows no rate-dependency (<1% per ten-fold change in shear velocity *v*).

## 3.1. Material tested

The tested bulk material consists of quartz sand SIBELCO S80 with grain size of ~0.63-355 µm (D50 = 175 µm. Bulk and grain densities are 1300 kg/m³ and 2650 kg/m³, respectively and the hardness is 7 on Moh's scale. S80 is sold e.g., by the company SIBELCO (sibelco.com).

## 3.2. Measurement procedure

The data presented here are derived by ring shear testing using a SCHULZE RST-01.pc (Schulze, 1994, 2003, 2008) at *HelTec*, the Laboratory for experimental tectonics at the Helmholtz Center Potsdam – GFZ German Research Centre for Geosciences in Potsdam, Germany. The RST is specially designed to measure friction coefficients $\mu$ and cohesions $C$ in loose granular material accurately at low confining pressures (<20 kPa) and shear velocities (<1 mm/sec) similar to analogue experiments. In this tester, a granular bulk material layer is sheared internally at constant normal stress $\sigma_N$ and shear velocity $v$ while shear force and lid displacement (corresponding to density and volume change $\Delta V$) are measured continuously. For more details see Klinkmüller et al. (2016).

### 3.2.1. Sample preparation and test conditions

Each sample is carefully prepared by the same person and measured consistently following the same protocol (Table 1). The measurements presented here correspond to internal friction, i.e. shearing inside the material. Preparation includes sieving the material (using the "Geomod" sieve) at a rate of ca. 30 g/min/cm² from about 30 cm height into a shear cell of type No. 1. The bulk density reached with this procedure is 1552±7 kg/m³. Normal force, shear force, shear velocity and lid displacement are measured at 5000 Hz (VST) and then down sampled to 5 Hz. Laboratory conditions are air conditioned during all the measurements (temperature: 22°C, humidity: 40%). The tests are documented under the GFZ Lab-IDs 577-01 (Table 1).

*Table 1: Sample overview*

| GFZ-ID | Material | Preparation | Procedure |
|---|---|---|---|
| 577-01 | Quartz sand SIBELCO S80 | Sieved (Geomod) | RST |
| 577-01 | Quartz sand SIBELCO S80 | Sieved (Geomod) | VST |

### 3.2.2. RST (Ring-shear test) procedure

During RST a shear velocity of $v$ = 30 mm/min and a series of normal loads are imposed while shear force and lid displacement are measured. 18 individual tests are done at normal stresses of $\sigma_N$ = 500, 1000, 2000, 4000, 8000, and 16000 Pa (with 3 repetitions per stress level). During the measurement the material is sheared for initially 3 minutes (90 mm of displacement). During this period the shear stress $\tau$ reaches a peak (= peak friction) and then drops to a plateau indicating shear has localized into a shear zone (= dynamic friction). The sample is then unloaded by shortly reversing rotation (at 10 mm/min) and immediately re-sheared for 3 minutes during which shear stress $\tau$ reaches a second peak (= reactivation friction) before returning to the plateau simulating reactivation of an existing shear zone. The RST has been run under the GFZ Lab-ID 577-01.

### 3.2.3. VST (Velocity stepping test) procedure

To determine the dependence of friction on the shear velocity $v$, a velocity stepping test (VST) is performed. During VST shear velocities ranging from $v$ = 0.1 to $v$ = 30 mm min$^{-1}$ and a normal stress of $\sigma_N$ = 2000 Pa are imposed (Table 2). Velocity is systematically decreased in logarithmic steps of individual time lengths adapted to the respective velocity to reach a comparable displacement of 10 mm in each step (Table 3). The velocity steps are applied after having reached the plateau of the dynamic friction during a 3 minutes pre-shear phase. The VST has been run under the GFZ Lab-ID 577-01.

*Table 2: VST conditions*

| **Normal stress [Pa]** | **Shear velocity *v* [mm/min]** | **Period *T* [hh:mm:ss]** |
|---|---|---|
| 2000 | 30 | 00:00:20 |
| 2000 | 10 | 00:01:00 |
| 2000 | 3 | 00:03:20 |
| 2000 | 1 | 00:10:00 |
| 2000 | 0.3 | 00:33:20 |
| 2000 | 0.1 | 01:40:00 |

## 3.3. Analysis method

The raw data are here analyzed and visualized using the customized open-source software package "RST-Evaluation" (Rudolf and Warsitzka, 2019).

### 3.3.1. RST analysis: Friction coefficients and cohesion

In a first step, shear curves (Figure 1) are constructed by converting forces to stresses and time to displacement. Then, three characteristic values (strengths) are picked automatically (and revised manually if necessary) from the shear curves:

(1) The **peak shear strength $\tau_P$** during the first peak in the shear curve representing initial strain localization
(2) the **dynamic shear strength $\tau_D$** on the plateau after localization representing friction during sliding
***(3)*** the **reactivation shear strength $\tau_R$** during the second peak representing static friction during reactivation of the shear zone.

We then perform regression analysis of these friction data by means of linear regression in two ways:

- A linear regression through all data pairs of shear strength $\tau^*$ and normal stress $\sigma_N$ (Figure 2). The slope of the linear regression corresponds to the friction coefficient $\mu$ and the y-axis intercept to cohesion *C*. This method assumes that the material behaves strictly as a Mohr-Coulomb material, i.e., has a linear failure envelope.

- Calculating all possible two-point slopes (friction coefficient $\mu$) and y-axis intercepts (cohesion *C*) for mutually combined data pairs of shear strength $\tau^*$ and normal stress $\sigma_N$ (Figure 3). These data (i.e., all individual $\mu$ and *C*) are then evaluated by means of univariate statistics by calculating mean and standard deviation and comparing the probability density function (pdf) to that of a normal distribution. This method overcomes the limitation of the analysis to Mohr-Coulomb material and allows for non-linear failure envelopes (Santimano et al., 2015).

In case values for $\mu$ and *C* as derived from the two methods are identical (within standard deviation), the material is properly characterized by a straight Mohr-Coulomb failure envelope.

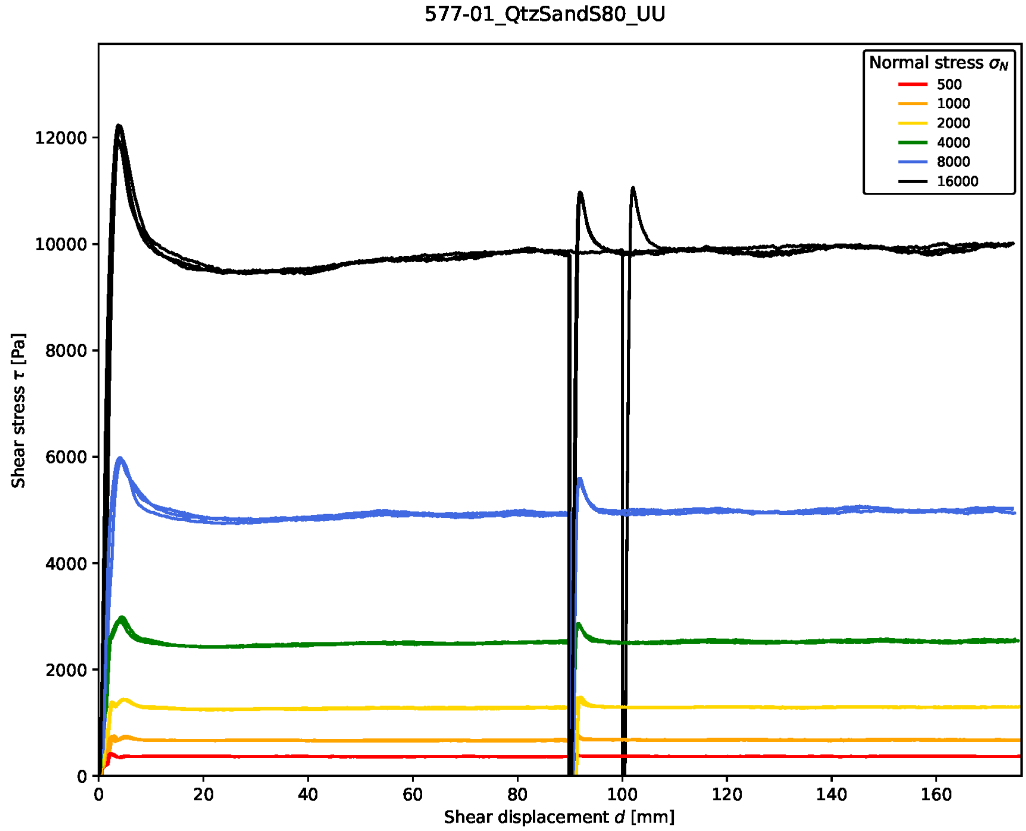


*Figure 1: **RST shear curve (577-01_ts.pdf).** Y-axis is shear stress τ, x-axis is shear displacement d. Each data set consists of 18 shear curves corresponding to 6 levels of normal stress $\sigma_N$ with 3 repetitions of each stress level.*

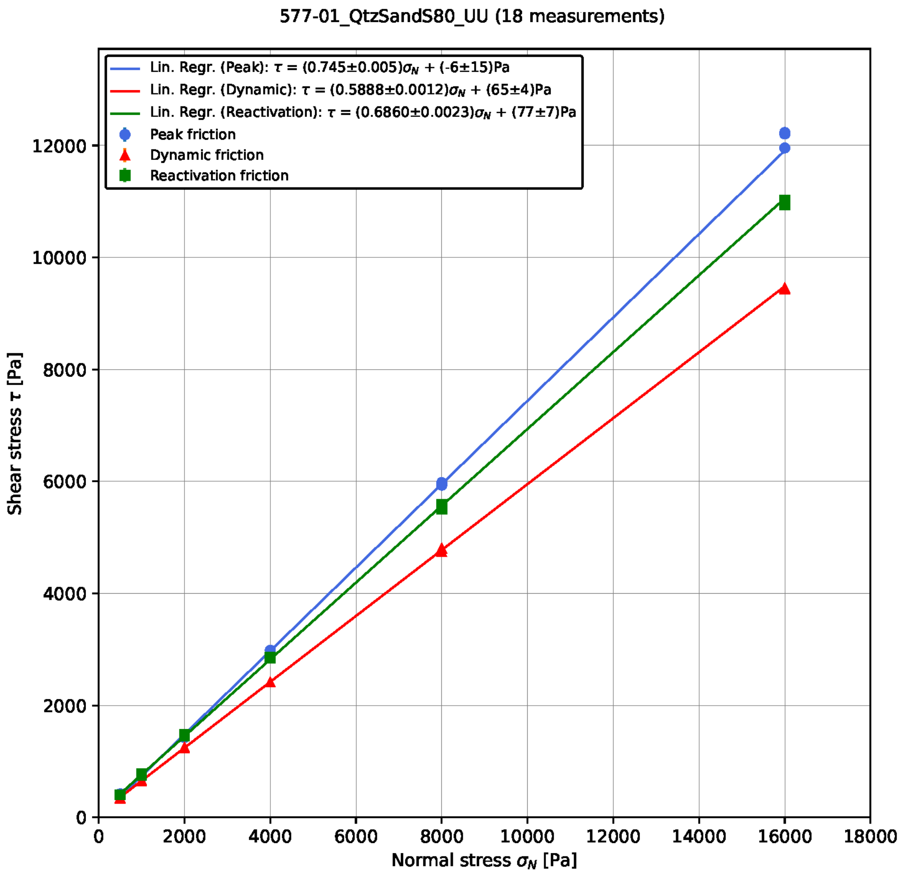


*Figure 2: **RST linear regression (577-01_linregr.pdf).** Plot of all data pairs in the Mohr space (normal stress $\sigma_N$ vs. shear stress τ) including curves of the corresponding linear least-squares regression.*

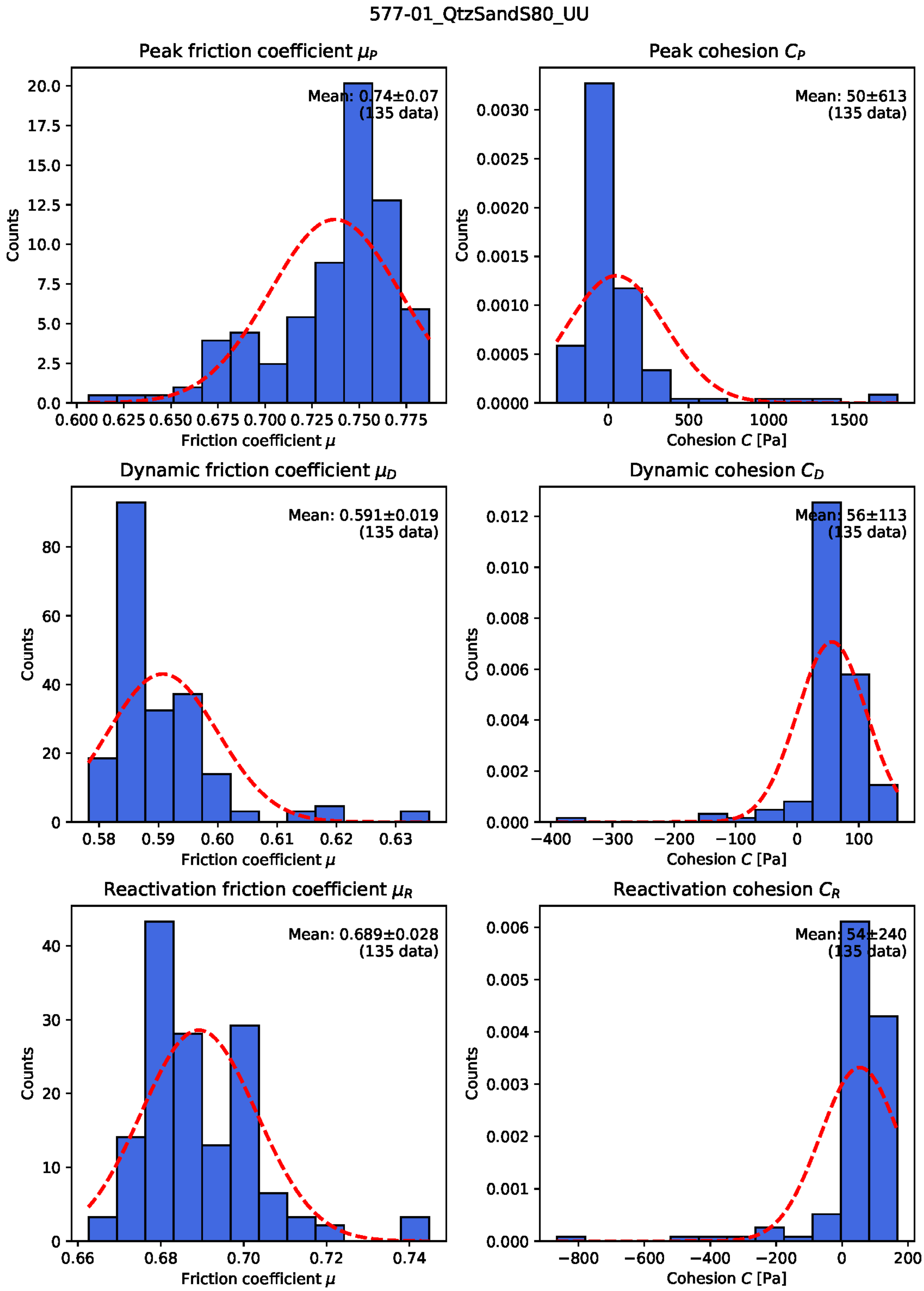


*Figure 3:* ***RST mutual regression histograms (577-01_hist.pdf).*** *Histograms of mutual two-point regression results for slope (friction coefficient μ) and y-axis intercept (cohesion C). Red curves are synthetic normal distributions with the same mean and standard deviation (std.) as the data set for comparison*

### 3.3.2. VST analysis: Rate-dependency of dynamic friction

From the VST time-series data apparent friction (shear stresses $\tau$ normalized by normal stress $\sigma_N$) are plotted as a function of log($v$) (Figure 4). Note, that friction can be systematically overestimated here because cohesion is not considered. For regression analysis, the 20 percentile "fit data" are used in order to reduce the weight of extreme values. The slope of the regression then reflects the rate dependency of dynamic friction.

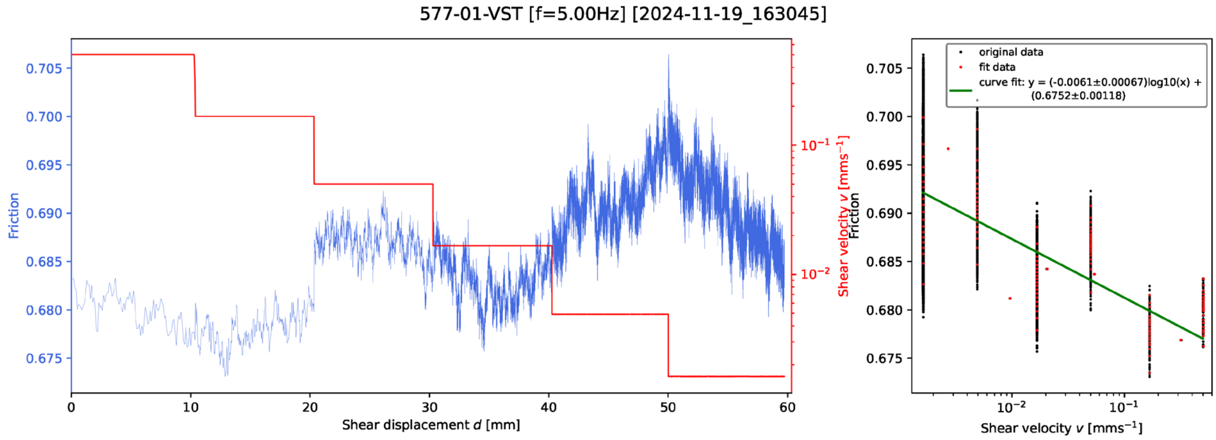


*Figure 4: **VST data and regression (577-01_VST.pdf)**. The shear velocity v is decreased stepwise (red curve), while the dynamic friction (shear stress τ/normal stress σN) is measured (blue curve). The logarithmic fit (green curve) through the "fit data" reflects the slight decrease of the friction with increasing shear velocity v.*

# 4. File description

There exist the following files in the zipped folder "2024-xxx_RST" and subfolders:

(i) RST raw data ("577-01-X.tdms") with X = 01-18
(ii) RST shear curve data ("577-01_ts.txt"; example Table 3)
(iii) RST shear curve plot ("577-01 _ts.pdf"; example Figure 2)
(iv) RST friction data ("577-01_peak.txt", "577-01_dynamic.txt", "577-01_reactivation.txt"; example Table 4)
(v) RST friction plot and linear regression data ("577-01_linregr.pdf", "577-01_fricstd.txt"; example Figure 3)
(vi) RST histograms of friction data and mutual linear regression data ("577-01_hist.pdf", "577-01_fricmut.txt"; example Figure 4)
(vii) VST raw data ("577-01_VST.tdms")
(viii) VST plot ("577-01_VST.pdf"; example Figure 4)

Raw data (i) and (vii) are stored in subfolder "2024-xxx_RSTdata". Data products (ii)-(vi) and (viii) are stored in subfolder "2024-xxx_RSTproducts". An overview of all files of the data set is given in the file "2024-xxx_LoF.pdf".

## 4.1. RST data and products

RST shear curve data are derived from RST raw data (i) and given as time series (ts) data (ii) in .txt-format (Table 3) and visualized as shear curves (iii) (Figure 1). Note that the conversion from forces in raw data to stresses depends on various machine specific parameters (e.g. shear cell geometry) not explicitly reported here. In case of interest please contact the authors.

*Table 3:* ***Example of RST shear curve time series data (577-01_ts.txt).*** *First line is header. First column is time (in s). Columns 2-13 are shear forces (in N) for corresponding normal stresses as specified in the header of the respective columns (4 normal stress levels from 500 to 16000 Pa, three repetitions per stress level).*

| **Time [s]** | **500** | **1000** | **2000** | **…** |
|---|---|---|---|---|
| 0.00000 | -4.90 | 70.58 | -5.27 | … |
| 0.20000 | … | … | … | … |
| … | … | … | … | … |

RST friction data (iv) are provided as data pairs (normal stress $\sigma_N$ and shear strength $\tau^*$; Table 4) for peak, dynamic and reactivation friction in txt format. They are visualized and analysed (v) by plotting into Mohr Space (normal stress $\sigma_N$ vs. shear stress $\tau$) and performing a linear regression (Figure 2), the results of which are stored in .txt-format. The results of the mutual regression analysis (see 2.3) are plotted in histograms (vi) for friction coefficients $\mu$ and cohesions $C$ (Figure 3), with the data additionally given in .txt-format.

*Table 4:* ***Example of RST data (577-01_peak.txt).*** *First line is header. First column is normal stress $\sigma_N$ (in Pa). Second column is shear strength $\tau^*$(in Pa).*

| **Normal stress [Pa]** | **Shear strength [Pa]** | **Stddev.Shear strength [Pa]** |
|---|---|---|
| 500 | 410 | 10 |
| 1000 | … | … |
| … | … | … |

### 4.2. VST data and products

VST raw data (vii) and analysis results are visualized (viii) by first plotting shear velocity $v$ and apparent dynamic friction (shear stress $\tau$ divided by normal stress $\sigma_N$) against the shear displacement $d$ and secondly in a plot of apparent dynamic friction vs. log($v$) including the regression (Figure 4).

## 5. Results

According to our analysis the material shows a Mohr-Coulomb behaviour characterized by a linear failure envelope. Peak, dynamic and reactivation friction coefficients of corundum sand are µP = 0.75, µD = 0.59, and µR = 0.69, respectively (Table 5). Cohesion of the material ranges between 0-80 Pa. The material shows no rate-dependency (<1% per ten-fold change in shear velocity v).

*Table 5: Summary of RST data*

| Parameter | Symbol | Unit | Linear least-squares regression method | | Mutual two-point regression method | |
|---|---|---|---|---|---|---|
| | | | Value | Standard deviation | Value | Standard deviation |
| Coefficient of peak friction | $\mu_P$ | - | 0.745 | 0.005 | 0.740 | 0.070 |
| Peak cohesion | $C_P$ | Pa | -6 | 15 | 50 | 613 |
| Coefficient of dynamic friction | $\mu_D$ | - | 0.589 | 0.001 | 0.591 | 0.019 |
| Dynamic cohesion | $C_D$ | Pa | 65 | 4 | 56 | 113 |
| Coefficient of reactivation friction | $\mu_R$ | - | 0.686 | 0.002 | 0.689 | 0.028 |
| Reactivation cohesion | $C_R$ | Pa | 77 | 7 | 54 | 240 |
| Rate dependency | $\Delta\mu_D/\Delta \log v$ | % | -0.61 | 0.01 | n.a. | n.a. |

## 6. References

Klinkmüller, M., Schreurs, G., Rosenau, M., & Kemnitz, H. (2016). Properties of granular analogue materials: A community wide survey, Tectonophysics, 684, 23-38, https://doi.org/10.1016/j.tecto.2016.01.017

Rudolf, M. & Warsitzka, M. (2019): RST Evaluation - Scripts for analysing shear experiments from the Schulze RST.pc01 ring shear tester, http://doi.org/10.5880/GFZ.4.1.2021.001

Santimano, T., Rosenau, M., & Oncken, O. (2015). Intrinsic versus extrinsic variability of analogue sand-box experiments – Insights from statistical analysis of repeated accretionary sand wedge experiments. Journal of Structural Geology, 75, 80–100, https://doi.org/10.1016/j.jsg.2015.03.008

Schulze, D. (1994). Entwicklung und Anwendung eines neuartigen Ringschergerätes. Aufbereitungstechnik, 35 (10), 524-535

Schulze, D. (2003). Time-and Velocity-Dependent Properties of Powders Effecting Slip-Stick Oscillations. Chemical Engineering & Technology, 26(10), 1047-1051, https://doi.org/10.1002/ceat.200303112

Schulze, D. (2008). Powders and Bulk Solids - Behavior, Characterization, Storage and Flow, Springer Berlin Heidelberg New York, ISBN 978-3-540-73767-4, 511 pp. https://doi.org/10.1007/978-3-540-73768-1